Talanta 97 (2012) 388–394

Contents lists available at SciVerse ScienceDirect

Talanta

journal homepage: www.elsevier.com/locate/talanta

Simple and rapid colorimetric detection of Hg(II) by a paper-based device using silver nanoplates

Amara Apilux [a], Weena Siangproh [b], Narong Praphairaksit [a,c], Orawon Chailapakul [a,c,*]

[a] Electrochemistry and Optical Spectroscopy Research Unit, Department of Chemistry, Faculty of Science, Chulalongkorn University, 254 Phayathai Road, Pathumwan, Bangkok 10330, Thailand
[b] Department of Chemistry, Faculty of Science, Srinakharinwirot University, Sukhumvit 23, Wattanna, Bangkok 10110, Thailand
[c] Center for Petroleum, Petrochemicals and Advanced Materials, Chulalongkorn University, 254 Phayathai Road, Pathumwan, Bangkok 10330, Thailand

ARTICLE INFO

Article history:
Received 6 March 2012
Received in revised form
19 April 2012
Accepted 24 April 2012
Available online 14 May 2012

Keywords:
Mercury
Silver nanoparticles
Nanoplates
Paper-based device

ABSTRACT

This work combines lab-on-paper methodology with nanoparticle science to develop a new tool for the simple and rapid determination of Hg(II). The resulting paper-based device enables measurement of Hg(II) from only 2 μL of sample solution. The color of the nanosilver in the test area immediately changes in the presence of Hg(II), and this change can be monitored by the naked eye. This method exhibits superior selectivity towards Hg(II) compared with the other metal ions tested. Furthermore, the results show a significant increase in the Hg(II) analytical signal when Cu(II) is added to the Ag Nanoplates at the test zone. With digital camera imaging and software processing, which are shown to further improve the quantitative capability of this technique, the linear detection range is 5–75 ppm Hg(II) with a limit of detection of 0.12 ppm. Using a pre-concentration scheme (based on repeated 2 μL applications of the test Hg(II) solution onto the same test zone) reduces the limit of detection to 2 ppb. The technique developed by this study provides a rapid, sensitive and selective detection method for aqueous Hg(II) samples and is especially suitable for remote field and environmental analysis.

1. Introduction

Mercury is highly toxic, and mercury exposure has severe adverse effects on human health and the environment. Environmental mercury contamination has several sources, including metal mining, industrial wastes, bleach production, agricultural pesticides, and volcanic activity. Mercury exists in the following three principal forms: elemental or metallic mercury (Hg(0)), ionic mercury salts (Hg(II)) (e.g., mercuric chloride) and organic compounds (e.g., methyl-, dimethyl- and phenyl-mercury) [1]. Because of its solubility in water, which provides a pathway for contaminating large amounts of water, Hg(II) is one of the most common and stable forms of mercury pollution. By this means, Hg(II) can accumulate in vital organs through the food chain and cause severe damage to the brain, nervous system, kidneys, heart and endocrine system [2]. Therefore, it is very important to routinely monitor Hg(II) ion levels in the environment. Due to its high toxicity, the United States Environmental Protection Agency (USEPA) limits mercury in drinking water to 0.002 mg/L [3]. Likewise, 0.005 mg/L is the maximum mercury level permitted by the industrial effluent standards set by the pollutant control department in Thailand [4]. Detection of Hg(II) has been accomplished using a variety of methods, including cold-vapor atomic absorption spectrometry [5,6], cold-vapor inductively coupled plasma mass spectroscopy [7], resonance scattering spectroscopy [8] and atomic fluorescence spectrometry [9–11]. Although these methods provide low limits of detection (LOD), they are sophisticated, time-consuming, high-cost operations that require complicated non-portable equipment and are, consequently, not suitable for field monitoring. Thus, there is a clear need for a simple, rapid, highly sensitive and selective method for Hg(II) detection in the field.

Because paper-based device methodologies are easy to use, rapidly implemented, inexpensive, and portable [12–14], there has been considerable interest of late in using such methods for environmental and clinical analyses. This kind of paper-based device, which can be used for colorimetric assays, uses a simple fabrication method that creates a hydrophobic wall that contains and/or directs a fluid analyte into the detection area. The wax screen-printing method is a particularly attractive procedure for creating large-volume and moderate-resolution paper-based devices [15]. This method's predominant advantages are its low cost, rapid detection and ease of fabrication as well as the fact that creation of the hydrophobic wall does not require solvent or

* Corresponding author at: Electrochemistry and Optical Spectroscopy Research Unit, Department of Chemistry, Faculty of Science, Chulalongkorn University, 254 Phayathai Road, Pathumwan, Bangkok 10330, Thailand. Tel.: +66 2 218 7615; fax: +66 2 218 7615.
E-mail address: corawon@chula.ac.th (O. Chailapakul).

0039-9140/$ - see front matter © 2012 Elsevier B.V. All rights reserved.
http://dx.doi.org/10.1016/j.talanta.2012.04.050

external processing steps. For these reasons, the present study used the screen-printing method.

Several recent detection studies have utilized noble metallic nanoparticles (NPs), such as gold (Au) or silver (Ag), as colorimetric sensors for the detection of Hg(II). Unfortunately, most of these methods require expensive and complicated chemical syntheses and surface modifications of the NPs using specific sensing materials, such as rhodamine B [16], aptamer [17], thymine [18] L-cysteine [19] oligonucleotides [20], thiol compounds [21] and mercaptopropionic acid [22]. Because of their lower cost compared with gold nanoparticles (AuNPs), the use of silver nanoparticles (AgNPs) in colorimetric sensors has become popular [23,24]. The molar extinction coefficient of AgNPs is also approximately 100-fold greater than that of AuNPs of the same size, resulting in improved visibility (due to the differences in optical brightness) and, therefore, increased sensitivity. This work aimed to develop a colorimetric method for the simple and rapid detection of Hg(II) ion levels using AgNPs and Ag nanoplates (AgNPls) on a paper-based device.

2. Experimental section

2.1. Chemicals and materials

Filter paper (No. 1, 125 cm diameter) was obtained from Whatman. Silver nanoparticles (AgNPs) with a diameter of 10 nm and silver nanoplates (AgNPls) with diameters of roughly 30, 35, 45 and 50 nm were obtained from the Sensor Research Unit at the Department of Chemistry, Chulalongkorn University. Syntheses of AgNPs and AgNPls employed a facile method that used starch as the stabilizer without capping agents. Analytical-grade reagents and 18 MΩ cm resistance deionized water (obtained from a Millipore Milli-Q purification system) were used throughout. A standard solution of 1000 ppm Hg(II) was purchased from Fluka, Switzerland, and used as the stock solution. The following chemicals were used as received: iron sulfate heptahydrate ($FeSO_4 \cdot 7H_2O$) (Merck), magnesium sulfate ($MgSO_4$) (Scharlau), nickel sulfate ($NiSO_4$) (Carlo Erba), lead sulfate ($PbSO_4$) (Unilab), cadmium sulfate ($CdSO_4$) (Baker Analyzed), zinc sulfate ($ZnSO_4$) and copper sulfate ($CuSO_4$) (BDH).

2.2. Fabrication of patterned paper

Paper-based devices were made from filter paper having hydrophobic walls constructed in specific patterns. In the system used herein, the pattern was designed with Adobe Illustrator software (Adobe Systems, Inc.), and the block screen was fabricated by Chaiyaboon (Bangkok, Thailand). Each test zone was comprised of 38 circles, each with a radius of 0.6 cm, per piece of filter paper [Fig. S1]. It is worth noting that other formats, such as linear strips and even rectangular arrays suitable for automation, can be printed and handled just as effectively. To fabricate the hydrophobic walls, solid wax (purchased from a local stationery store) was rubbed through the finely perforated screen onto the filter paper, after which the printed wax was melted on a hot plate at 100 °C for 30 s to allow the wax to be absorbed into the paper. When cooled to room temperature, this absorbed wax formed the hydrophobic barrier within the paper.

2.3. Colorimetric measurement of Hg(II)

The absorption spectra of the AgNPs and variously sized AgNPls were obtained with a UV–vis absorption spectrometer (HP HEWLETT PACKARD 8453) following the addition of different concentrations of Hg(II).

2.4. Hg(II) detection utilizing the AgNP/AgNPl paper device

A 2 μL suspension of 100 ppm nanosilver (either AgNPs or AgNPls) was applied to the middle of the hydrophilic test spot on the paper-based device. After the suspension of AgNPs or AgNPls was dried, 2 μL of either the test solution or an Hg(II) standard solution (of known concentration) was applied to this test zone. The AgNPs/AgNPls clearly changed color, an observation that could be made with the naked eye, almost immediately after the addition of the Hg(II) solution. An image processing technique was subsequently adopted to further differentiate the color changes and to improve the method's colorimetric capabilities. To this end, a picture of the paper-based device was taken by a digital camera (Cannon EOS 1000 D1, Japan) in a light control box (OPPLE 8 W daylight lamp). The image was then imported into Adobe Photoshop software, and the color signal in each test zone was measured as the mean color intensity. The readings obtained were used to generate the calibration curve. To improve the sensitivity, after the suspension of AgNPls was dried on the filter paper, various volumes (0–2 μL) of a 500 ppm $CuSO_4$ solution were applied to the test zone. The test or standard solution was then applied to the hydrophilic zone, and the reagents were allowed to react and air dry.

For quantitative analysis, standard reference solutions (with Hg(II) concentrations ranging from 0.1–100 ppm) were prepared and applied to the test zone, and, after 45 min, digital images were obtained. For each Hg(II) concentration, the signal intensity was measured and used to plot the calibration curve. The limits of detection (LOD) and quantification (LOQ) were calculated using 3 and 10 times the standard deviation of the blank measurements ($n=10$), respectively.

The Hg(II) selectivity of this new lab-on-paper method was investigated by comparing the signal intensities obtained for seven other metal ions, As(III), Ni(II), Fe(III), Cu(II), Zn(II), Mg(II), Cd(II) and Pb(II), over a concentration range of 5–500 ppm.

2.5. Scanning electron microscopy (SEM)

The reaction between AgNPs or AgNPls and Hg(II) on the paper-based device were further characterized using scanning electron microscopy (SEM). An image was captured after applying the test or standard Hg(II) solution to the test zone. The sample was then prepared by cutting the reaction zone of the paper-based device and attaching it to conductive adhesive tape. Finally, the prepared sample was splutter coated with gold and analyzed by SEM, and the Ag particle sizes were measured.

2.6. Evaluation of Hg(II) levels in real water samples

The drinking water sample (Singha, Singha Corporation) was purchased from a local supermarket, and the tap water sample was collected from a domestic drinking water supply in Bangkok after first discharging the standing tap water for 15 min and then boiling the collected sample for 10 min (to remove chlorine).

3. Results and discussion

3.1. Colorimetric detection of Hg(II)

Maximum absorption of the AgNPs that had a mean diameter of 10 nm occurred at approximately 400 nm, whereas the maximum absorption signals of AgNPls having mean diameters of 30, 35, 45 and 50 nm occurred at approximately 500, 525, 550 and 600 nm, respectively. We first evaluated the effects of particle size (for AgNPls vs. AgNPs) on the Hg(II) detection capabilities of the

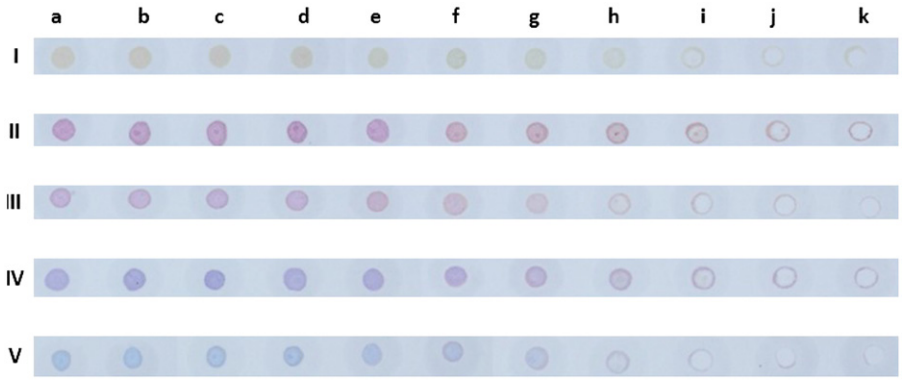

Fig. 1. Color changes of AgNPs and AgNPls in the presence of Hg(II) at concentrations of (a) 0, (b) 0.01, (c) 0.05, (d) 0.1, (e) 0.5, (f) 1, (g) 5, (h) 10, (i) 25, (j) 50 and (k) 100 ppm with 2.00 μL of a 100 ppm solution of AgNPs (10 nm diameter) or AgNPls with diameters of (II) 30, (III) 35, (IV) 45 and (V) 50 nm. Image shown is representative of those seen in three independent repeats. (For interpretation of the references to color in this figure legend, the reader is referred to the web version of this article.)

paper-based device. For both AgNPs and AgNPls, the test-area color suddenly changed when Hg(II) was applied (Fig. 1). This color change was easily observed with the naked eye for Hg(II) levels above 5 ppm for all AgNPls and AgNPs investigated. When the concentration of Hg(II) was increased from 1 to 25 ppm, the color of the test zone changed from yellow to light yellow for the AgNPs (~10 nm diameter) and from violet to pinkish orange, pinkish violet to pinkish yellow, dark blue to pinkish violet and blue to pinkish blue for the AgNPls with diameters of 30, 35, 45 and 50 nm diameter, respectively. In all cases, the test-area colors faded at Hg(II) levels above 25 ppm and were imperceptible when Hg(II) concentrations approached 100 ppm.

Digital images of each test zone were obtained, cropped and analyzed (using Adobe Photoshop software) to determine the mean color intensity value for each Hg(II) concentration tested. Each mean intensity value was then plotted against the concentration of Hg(II) [Fig. S2]. The signal intensity increased with increasing Hg(II) concentrations from 1–100 ppm for the 10 nm AgNPs and 30 nm AgNPls and from 0.5 to 100 ppm for the larger AgNPls. The curve was essentially linear in the 5–25 ppm range for the AgNPs (correlation coefficient (R^2)=0.983). Calibration curves were essentially linear in the range of 5–25 ppm (R^2=0.998), 5–50 ppm (R^2=0.996), 5–25 ppm (R^2=0.997) and 5–25 ppm (R^2=0.980) for AgNPls with diameters of 30, 35, 45 and 50 nm, respectively.

This phenomenon can be attributed to changes in the surface plasmon resonance (SPR) of the NPs/NPls, which is related to their apparent color. The color change of AgNPs, 10 nm in diameter with spherical shape, in the presence of Hg(II) is due to the reducing of their particle size. Whereas, the decomposition of silver nanoplates (AgNPls), which has larger particle size with plate shape, is related to change both their shape and size providing a wider range of color changes. Additionally, the color change results obtained by AgNPls with plate shape can be more clearly seen with the naked eye than AgNPs with spherical shape. The 35 nm (diameter) AgNPls were selected for further evaluation because their color change (in response to Hg(II)) could be easily distinguished by the naked eye and because their Hg(II) calibration curves exhibited the widest linear concentration range.

3.2. Characterization of ~35 nm (diameter) AgNPls in the presence of Hg(II)

For characterization of ~35 nm (diameter) AgNPls in the presence of Hg(II), there are two techniques used. The first is spectroscopy (UV–vis) that was used to characterize AgNPls in solution while SEM was used for morphological characterization of paper-based devices containing AgNPls. The maximum absorbance

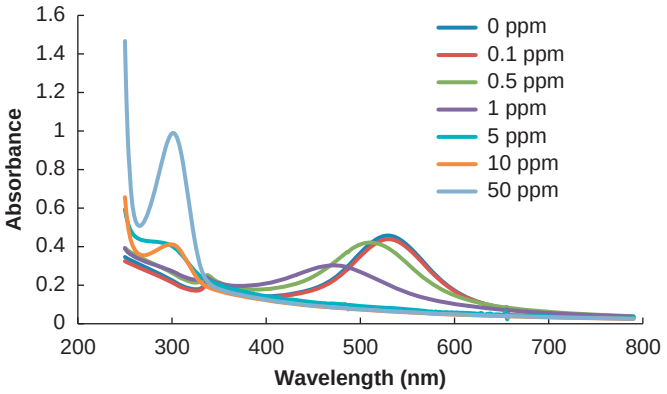

Fig. 2. The UV–vis spectra of 35 nm diameter AgNPls at 10 ppm after the addition of Hg(II) at different final concentrations.

of these AgNPls occurred at roughly 525 nm (Fig. 2), which could be ascribed to the SPR absorption of the AgNPls. The absorbance of the AgNPls at 525 nm progressively decreased as the concentration of Hg(II) ions increased and was no longer visible at Hg(II) levels above 5 ppm. Concurrently, the absorption peaks continually shifted towards shorter wavelengths with increasing Hg(II) concentrations. The visible color changes and absorption wavelength shifts suggest that the average particle size of the AgNPls decreased as the Hg(II) concentration increased. Additionally, the absorption spectrum of Ag(I), which exhibited an absorption maximum at approximately 300 nm, was clearly observed when the concentration of Hg(II) was higher than 5 ppm, indicating the oxidation of Ag(0) to Ag(I).

To verify the interaction between Hg(II) and the AgNPls, the AgNPls were examined by SEM. The resulting SEM images (Fig. 3) indicate that both the number and the average particle size of the AgNPls decreased after the addition of Hg(II) at 50 ppm. These results are consistent with the observed visible color change(s) and absorption shift(s) reported above. Thus, these phenomena can be ascribed to a redox reaction between the Hg(II) ions and the AgNPls. It appears that the AgNPs were oxidized by Hg(II), resulting in disintegration of the AgNPls into smaller particles, which changed their shape and consequently altered their SPR extinction band(s).

3.3. Selectivity of the 35 nm (diameter) AgNPls for Hg(II)

The selectivity of the 35 nm (diameter) AgNPls for Hg(II) ions was evaluated by individually testing potentially interfering

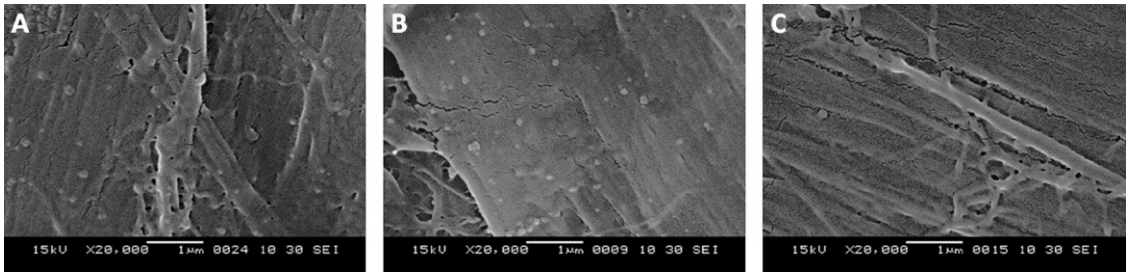

Fig. 3. Representative SEM images (20,000 × magnification) of (A) the 35 nm diameter AgNPls on the paper disc after exposure to 2 μL of Milli-Q water (B) AgNPls on the paper disc after exposure to 2 μL of 50 ppm Hg(II) and (C) 50 ppm Hg(II) on the paper disc.

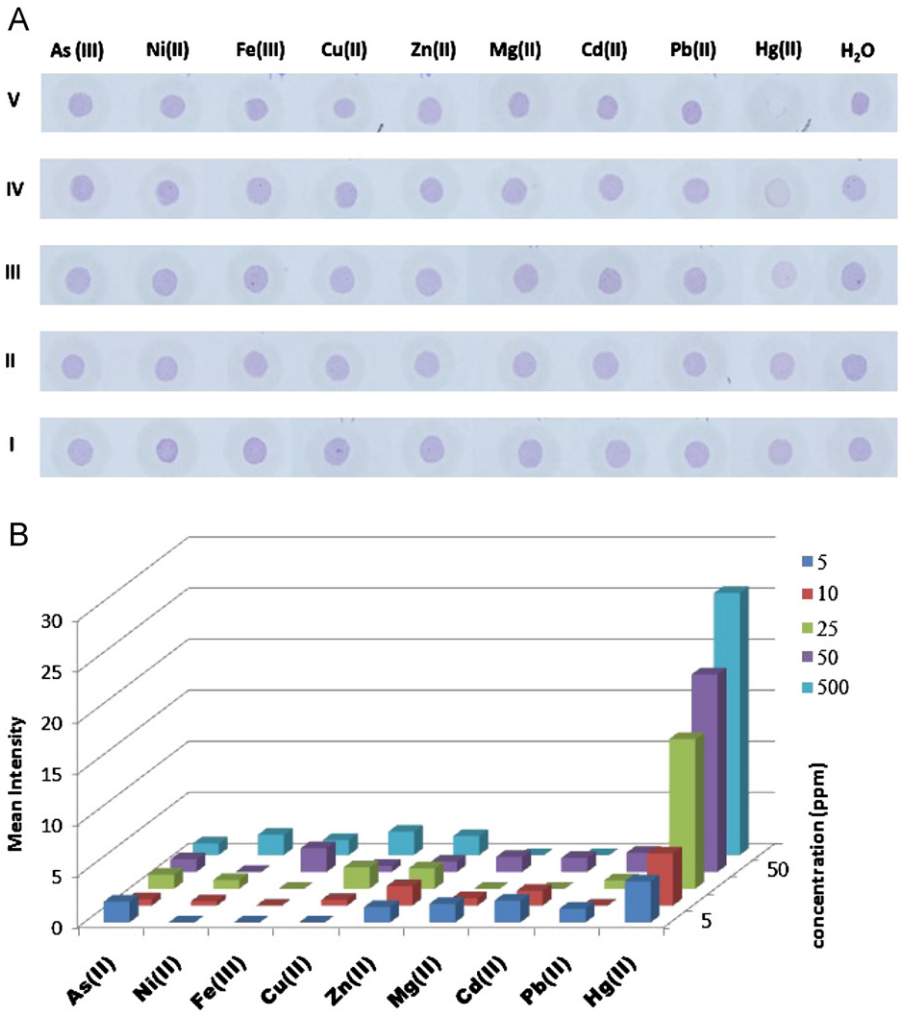

Fig. 4. Color changes of the 35 nm diameter AgNPls in the presence of the indicated metal ions, added as 2 μL of a (I) 5, (II) 10, (III) 25, (IV) 50, (V) 500 ppm solution. (A) A representative visual image of the paper device and (B) the mean intensity of the AgNPls' color determined by digital-image analysis using Adobe Photoshop. (For interpretation of the references to color in this figure legend, the reader is reffered to the web version of this article.)

metal ions, As(III), Ni(II), Fe(III), Cu(II), Zn(II), Mg(II), Cd(II) and Pb(II), at 5–500 ppm. Even at concentrations that were 100 times greater than that of Hg(II) (i.e., 500 ppm) all the other metal ions tested induced no obvious color changes (of the AgNPls, Fig. 4A). Furthermore, the more sensitive quantification method using mean color intensity values (of the AgNPls as determined by Adobe Photoshop analysis of digital images) revealed no significant detection of any of the test metal ions for concentrations up to 500 ppm (Fig. 4B). Only Hg(II) was found to significantly increase the AgNPl color intensity visualized with the naked eye. This finding is explained by the relatively high standard reduction potential of Hg^{2+} (E^0 $Hg^{2+}/Hg^0 = 0.85$ V) that can readily oxidize Ag^0 to Ag^+. All of the other metal ions tested have lower electrochemical potentials relative to Ag^0, thus, they have no apparent effects on the silver [25].

3.4. Effect of copper(II) ions on the Hg(II) detection by AgNPls

It is commonly reported that Copper(II) (Cu(II)) ions interfere with the electrochemical detection of mercury [26]. Moreover, Cu(II) can bind to aminothiol, resulting in the aggregation of AgNPs, which affects the color response [27]. Thus, the effect of

Cu(II) ions on Hg(II) detection was investigated by adding varying amounts (0–2 μL) of a 500-ppm Cu(II) solution to the test zone following the deposition of AgNPls and then assaying the color and intensity of the AgNPls upon application of Hg(II) in the range of 0.1–25 ppm. The results show that, for the same amount of Hg(II) applied, the color intensity of the test zone gradually increased with increasing amounts of added Cu(II) solution up to 1 μL, after which the response remained steady [Fig. S3]. Thus, the addition of 1 μL of 500 ppm Cu(II) was adopted for further experiments. This represents a 4.24 fold mole excess of Cu(II) to Ag(0) and a 9.5–190 fold mole excess of Cu(II) to Hg(II) for Hg(II) solutions of 5–100 ppm.

Subsequently, the effect of Hg(II) detection with or without Cu(II) (1 μL of 500 ppm) was compared (Fig. 5). The mean color intensity of the AgNPls in the presence of Hg(II) ions was significantly greater in the presence of Cu(II) than in the absence of Cu(II), and the LOD in the presence of Cu(II) was reduced such that a 0.1 ppm solution of Hg(II) could be readily detected. Despite the significant improvement in the analytical signal obtained in the presence of Cu(II), there were no significant changes in the color/shade of the AgNPls observed for each concentration of Hg(II).

The effect of Cu(II) on the AgNPs–Hg(II) interaction was evaluated by SEM, which revealed that the particle size (mean

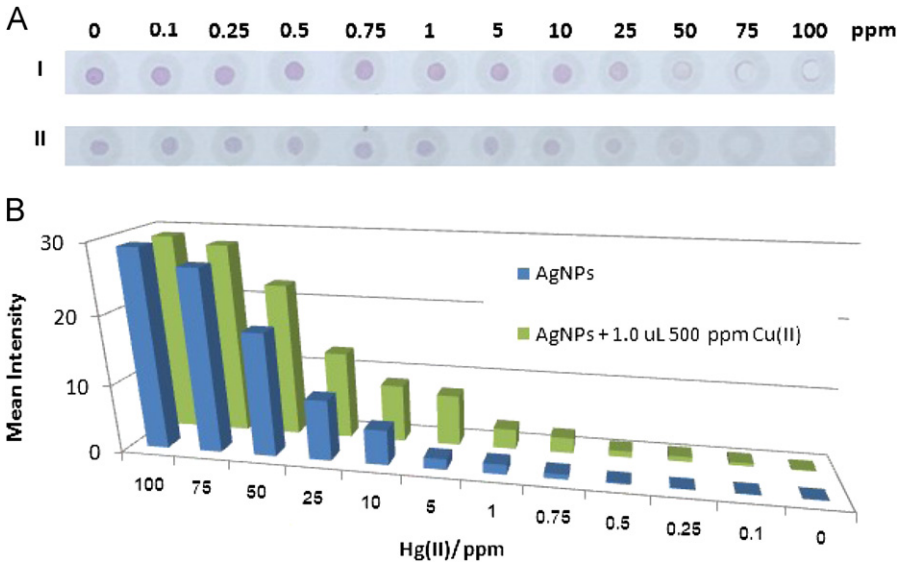

Fig. 5. Comparison of the color change of the 35 nm diameter AgNPls after the addition of 2 μL of Hg(II) at the indicated concentrations with or without the prior addition of 1 μL of 500 ppm Cu(II). (A) A representative visual image of the paper device (I) with or (II) without the addition of Cu(II) (B) the mean intensity of the AgNPls' color determined by digital-image analysis using Adobe Photoshop. (For interpretation of the references to color in this figure legend, the reader is reffered to the web version of this article.)

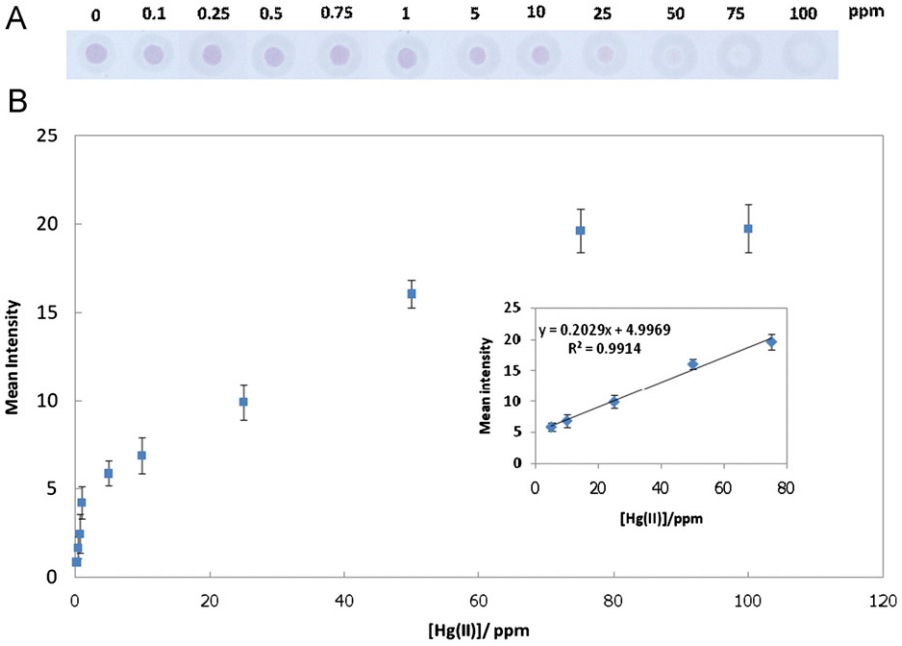

Fig. 6. Detection of Hg(II) in the range of 0–100 ppm in the presence of 1 μL of 500 ppm Cu(II) (applied in the preparation step). (A) A representative visual image of the paper device from three independent repeats; (B) the mean intensity of the AgNPls' color determined by digital-image analysis using Adobe Photoshop, plotted as an Hg(II) calibration curve. (Inset) Linear regression analysis and best fit line in the 5–75 ppm Hg(II) concentration range. (For interpretation of the references to color in this figure legend, the reader is reffered to the web version of this article.)

diameter) of the AgNPls in the presence of Cu(II) was similar to that seen in the absence of Cu(II) [Fig. S4]. However, in the presence of Cu(II), the average particle size of the AgNPls decreased upon addition of Hg(II), and the number of AgNPls was reduced to a greater extent (compared with results obtained in the absence of Cu(II)). Enhancement of the color signal may be due to the catalytic effect of Cu(II) on the redox reaction of Hg(II) with AgNPls to form Ag(I). The Cu(II) could cause the decrease in the reduction potential of the Ag(0) making Ag(0) more easily oxidized by Hg(II). In addition, the Cu(II) could form amalgam with Hg(II) and this amalgam can probably facilitate the oxidation of Ag(0) to Ag(I).

3.5. Calibration curve of Hg(II) detection by the 35 nm (diameter) AgNPls

A calibration curve was obtained by plotting the mean color intensity values (recorded from the Adobe Photoshop software analysis) versus the standard Hg(II) concentrations in the range of 0–100 ppm (Fig. 6). Reasonable linearity was obtained in the range of 5–75 ppm (R^2=0.991), with a LOD and LOQ of 0.12 ppm and 3.9 ppm, respectively. Clearly, the LOD requires enhancement for Hg(II) detection in real samples.

3.6. Pre-concentration of samples (multiple applications)

One advantage of lab-on-paper devices is that analyte pre-concentration, which enhances the signal intensity, can be easily obtained via multiple applications of the analyte sample to the test zone. Solutions containing less than 0.5 ppm Hg(II) can be readily determined using this pre-concentration scheme. For example, the method used in this study is clearly able to detect 50, 5 and 2 applications of 2 μL of 0.2, 2 and 5 ppm Hg(II) solutions, all of which resulted in signal intensities more or less equivalent to that obtained with a single 2 μL application of 10 ppm Hg(II) solution [Fig. S5]. The pre-concentration results show a percent recovery in the range of 95–114% and a reduction in the LOD to 0.2 ppm Hg(II) (Table 1), which makes the technique more applicable to real samples and use in the field of environmental science.

The minimum numbers of 2 μL applications of Hg(II) solution in which color changes are visually discernible were determined for five different Hg(II) concentrations in the 0.02–0.2 ppm range (Fig. 7). The color change was visibly distinguishable after 15, 30 and 30 applications of 2 μL of the 0.2, 0.1 and 0.075 ppm Hg(II) solutions, respectively. Using digital images and Adobe Photoshop analysis, a concentration of 0.1 ppm Hg(II) could be detected with only five 2 μL applications. For sample concentrations of less than 0.1 ppm, the number of applications could be increased to obtain a sufficient signal. Accordingly, the proposed method can be used to detect Hg(II) concentrations as low as 2 ppb, although this concentration requires 70 applications with 5 hours. The automatic dropper could be used instead of using manual pipette. Thus, pre-concentration (via repeated applications of the test sample onto the same test zone) successfully improved the LOD of this system.

Table 1
Determination of Hg(II) using the pre-concentration method (multiple applications of the test sample).

Hg(II)			
Added		Found	% Recovery
(ppm)	Applications	(ppm)	
0.2	1	ND	–
2	1	1.71 ± 0.41	86
5	1	5.68 ± 0.25	114
10	1	11.10 ± 0.37	111
0.2	50	9.49 ± 0.37	95
2	5	10.57 ± 0.42	106
5	2	11.01 ± 0.34	110

ND=not detected.

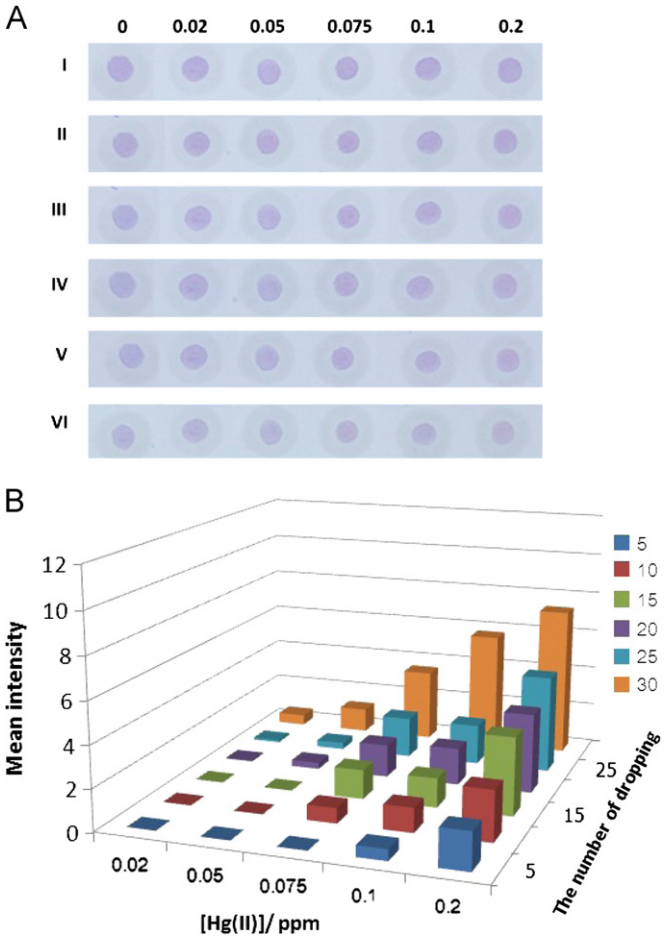

Fig. 7. Decreased LOD for Hg(II) levels obtained via in situ pre-concentration of the test sample (repeat 2 μL applications on the test zone) using the 35 nm AgNPls and the indicated Hg(II) concentrations. (A) A representative visual image of the paper device, from three independent repeats, showing (I) 5, (II) 10, (III) 15, (IV) 20, (V) 25 and (VI) 30 applications of 2 μL of the indicated Hg(II) concentration and (B) the mean intensity of the AgNPls' color determined by digital-image analysis using Adobe Photoshop. (For interpretation of the references to color in this figure legend, the reader is reffered to the web version of this article.)

3.7. Application of AgNPls on paper to detect Hg(II) levels in real water samples

The proposed paper-AgNPls/Cu(II) device for determination of Hg(II) ion levels was evaluated with two real water samples, one from commercially bottled drinking water and another from domestic tap water. Neither sample induced any visible color change in the AgNPls, indicating that the Hg(II) contents of these water samples were below 5 ppm. No color change was observed even after pre-concentration with 70 applications of the sample. Therefore, it can be concluded that the Hg(II) concentrations in these samples were below 2 ppb. The declared ICP-OES (a model iCAP 6000 series) analysis (detection limit of 2 ppb), also detected no Hg(II). When these water samples were spiked with different Hg(II) concentrations, the analytical recoveries were in the acceptable range of 96–103% and 90–113% for the bottled and

Table 2
Determination of Hg(II) levels in real water samples.

Sample	Hg(II) (ppm)		% Recovery	% RSD
	Added	Found		
Drinking water	0	ND	–	–
	1	1.03 ± 0.24	103	4.94
	5	4.78 ± 0.27	96	3.57
	10	9.60 ± 0.32	96	3.20
	25	24.71 ± 0.33	99	3.24
Tap water	0	ND	–	–
	1	0.89 ± 0.40	90	8.53
	5	4.57 ± 0.29	91	5.10
	10	9.20 ± 0.37	92	5.95
	25	28.35 ± 0.36	113	3.35

ND=not detected.

tap water, respectively, and exhibited precisions (% RSD) in the range of 3.2–4.9% and 3.3–8.6%, respectively (Table 2). The agreement between the detected and expected values suggests that it is likely that the Hg(II) levels in the two water samples are less than 2 ppb and that they have not been masked by their matrices. These findings thereby validate the detection method employed and demonstrate the potential of the method developed herein for the detection of Hg(II) in real water samples.

4. Conclusions

A colorimetric Hg(II) detection method using 35 nm diameter AgNPls on a paper-based device has been developed. The paper-based device is easily constructed using wax-screen printing, and Hg(II) can be easily detected with the naked eye via the resulting color change of the AgNPls (on the paper-based device) after a 2 μL application of the Hg(II) test solution. Digital imaging of the paper device and analysis using Adobe Photoshop software improves the sensitivity of the method from 5 ppm (obtained by the naked eye) to 0.1 ppm (LOD). The method has demonstrated good selectivity for Hg(II) against other metal ions, and the signal can be further enhanced with the addition of Cu(II). A significant reduction in the Hg(II) LOD (to as low as 2 ppb) is achieved by in situ pre-concentration (multiple applications of the test sample). Finally, the method developed herein has been successfully used to determine Hg(II) levels in real water samples.

Acknowledgements

A.A. gratefully acknowledges the Thailand Research Fund through the Royal Golden Jubilee Ph.D. Program (Grant No. PHD/0256/2549). OC greatly thanks the Thailand Research Fund, the Thai Government Stimulus Package 2 (TKK2555), under the Project for Establishment of Comprehensive Center for Innovative Food, Health Products and Agriculture, Chulalongkorn University and The National Research University Project of CHE and Ratchadaphiseksomphot Endowment Fund (Project Code AM1009I) and PCU013.2012. We gratefully acknowledge the financial support from the 90th Anniversary of Chulalongkorn University Fund (Ratchadphiseksomphot Endowment Fund). We also thank Prof. Dr. Sanong Ekgasit, Sensor Research Unit at the Department of Chemistry, Chulalongkorn University, for the silver nanoparticles.

Appendix A. supplementary material

Supplementary data associated with this article can be found in the online version at http://dx.doi.org/10.1016/j.talanta.2012.04.050.

References

[1] 〈http://www.chem.unep.ch/mercury/report/Final%20report/final-assessment-report-25nov02.pdf〉.
[2] Z. Gu, M. Zhao, Y. Sheng, L.A. Bentolila, Y. Tang, Anal. Chem. 83 (2011) 2324–2329.
[3] 〈http://water.epa.gov/drink/contaminants/basicinformation/mercury.cfm〉.
[4] 〈http://www.pcd.go.th/info_serv/en_reg_std_water04.html〉.
[5] Y. Zhang, S.B. Adeloju, Talanta 74 (2008) 951–957.
[6] K. Edyta, P. Krystyna, G. Slawomir, B. Ewa, Anal. Sci. 16 (2000) 1309–1312.
[7] J.L. Mann, S.E. Long, W.R. Kelly, J. Anal. At. Spectrosc. 18 (2003) 1293–1296.
[8] G. Wen, A. Liang, Z. Jiang, X. Liao, J. Li, H. Jiang, Luminescence 25 (2010) 373–377.
[9] Q.Q. Zhang, J.F. Ge, Q.F. Xu, X.Bo. Yang, X.Q. Cao, N.J. Li, J. Lu, Tetrahedron Lett. 52 (2011) 595–597.
[10] K. Leopold, M. Foulkes, P.J. Worsfold, Anal. Chem. 81 (2009) 3421–3428.
[11] M.J. Bloxham, S.J. Hill, P.J. Worsfold, J. Anal. At. Spectrosc. 11 (1996) 511–514.
[12] W.A. Zhao, A. van den Berg, Lab Chip 8 (2008) 1988–1991.
[13] W. Dungchai, O. Chailapakul, C.S. Henry, Anal. Chem. 81 (2009) 5821–5826.
[14] A. Apilux, W. Dungchai, W. Siangproh, N. Praphairaksit, C.S. Henry, O. Chailapakul, Anal. Chem. 82 (2010) 1727–1732.
[15] W. Dungchai, O. Chailapakul, C.S. Henry, Analyst 136 (2011) 77–82.
[16] C.C. Huang, H.T. Chang, Anal. Chem. 78 (2006) 8332–8338.
[17] L. Li, B. Li, Y. Qi, Y. Jin, Anal. Bioanal. Chem. 393 (2009) 2051–2057.
[18] X. Liu, X. Cheng, T. Bing, C. Fang, D. Shangguan., Anal. Sci. 26 (2010) 1169–1172.
[19] F. Chai, C.G. Wang, T.T. Wang, Z.F. Ma, Z.M. Su, Nanotechnology 21 (2010) 025501–025507.
[20] Y. Wang, F. Yang, X. Yang, ACS Appl. Mater. Interfaces 2 (2010) 339–342.
[21] Y.J. Du, J.L. Yan, M. Ni, B.A. Du, J. Iran. Chem. Res. 4 (2011) 87–91.
[22] C.C. Huang, H.T. Chang., Chem. Commun. 12 (2007) 1215–1217.
[23] W. Leesutthiphonchai, W. Dungchai, W. Siangproh, N. Ngamrojnavanich, O. Chailapakul, Talanta 85 (2011) 870–876.
[24] H. Li, Z. Cui, C. Han, Sens. Actuators, B 143 (2009) 87–92.
[25] E. Sumesh, M.S. Bootharaju, A.T. Pradeep, J. Hazard. Mater. 189 (2011) 450–457.
[26] F. Okcu, F.N. Ertas, H.I. Gokcel, H. Tural, Turk. J. Chem. 29 (2005) 355–366.
[27] L. Li, B. Li, Analyst 134 (2009) 1361–1365.